STUDY OF THE ENERGY SPECTRUM OF SECONDARY ELECTRONS ARISING FROM PASSAGE OF α PARTICLES AND FISSION FRAGMENTS THROUGH THIN FOILS

V. M. AGRANOVICH, D. K. DAUKEEV, Yu. V. KONOBEEV, and S. Ya. LEBEDEV

Submitted March 17, 1969

Zh. Eksp. Teor. Fiz. 57, 401–410 (August, 1969)

Results are presented of a study of the energy spectrum of secondary electrons arising from passage of α particles and fission fragments through a thin aluminum foil. The electron spectrum was measured by a time-of-flight method in which the time of origin of the emission was determined from the pulse produced by the primary particle (fission fragment or α particle). A description of the spectrometer and the measurement technique is presented. The results obtained are explained on the basis of the thermal spike theory.

1. INTRODUCTION

P. L. KAPITZA[1] proposed a thermal emission mechanism to describe the secondary electron emission (SEE) produced by bombardment of the surface of a solid by particles. He calculated the total number of emission electrons per fast ionizing particle (secondary emission coefficient) and compared the results of the calculation with experimental data. Although the thermal mechanism has subsequently been criticized repeatedly (see, for example, [2]), the question of its relative role nevertheless remains open. In clarification of this question, there is great interest in determination not only of such integral SEE characteristics as the SEE coefficient, but also in determination of the secondary electron energy spectrum.

In this connection, in a previous paper[3] we obtained theoretically the energy spectrum of emitted secondary electrons on the basis of a thermal approach to the SEE mechanism which took into account the dependence of the heat capacity and thermal conductivity of the electron gas on temperature; we also measured the spectrum of secondary electrons arising in passage of 5.5-MeV α particles through a 0.1-μ nickel foil, and made a comparison of theory with experiment. In this paper[3] it was shown that in the case of α particles with their relatively low value of specific ionization loss the thermal mechanism cannot explain the features of the SEE spectrum. Therefore it is of interest to study the SEE produced by fission fragments, which have almost an order of magnitude higher specific ionization than α particles. The present paper is devoted to presentation of the results of such a study.

Experiments on SEE produced by fission fragments can be divided into two groups, depending on the technique used (current or pulse). In the first case the vacuum tube, with a cathode covered with a fissionable material (usually U^{235}), is placed in the thermal neutron flux of a reactor and separate measurements are made of the current of fission fragments and the total current (the current of fragments plus the current of secondary electrons).[4,5] Such experiments provide the possibility of measuring the magnitude of SEE averaged over all types of fission fragments, over all angles, and over all depths of fragment emission from the cathode, and cannot provide the spectrum of secondary electrons from a specific fragment in a small solid angle and for a given angle of incidence of the fragment, which considerably hinders the theoretical interpretation of the results obtained. In the current method it is difficult to take into account the effect of secondary electrons ejected from the collector both by fragments and by γ and β rays arising in fission.

The pulse method, which has been described by Whitehead[6] and Stein and Leachman,[7] permits study of the SEE corresponding to a specific primary particle in the presence of a primary particle flux of complex composition. By this means, with a retarding-potential method, the first measurements were made of the integral energy spectrum of secondary electrons averaged over all types of fission fragments from Cf^{252},[6] and the SEE coefficients were measured for traversal and reflection for films of various material under the action of fission fragments.[7] The cylindrical electrostatic lens used by Whitehead,[6] to focus on the detector electrons which have overcome the retarding potential, can distort the true energy spectrum and requires some interpretation, particularly in regard to the angular distribution of the secondary electrons.

The electrostatic analyzer method used in our previous work[3] does not permit recording the secondary electron spectrum with good resolution for small primary fluxes, since the improvement of the resolution in this method is limited by the electron detector noise. Therefore it was decided to use for recording the secondary electron spectrum a time-of-flight method with correlation with the accompanying particle, of the type successfully used in nuclear physics for neutron spectrometry. Recently this method has been used to record the spectra of photoelectrons and thermionic electrons.[8,9]

2. EXPERIMENTAL APPARATUS AND METHOD OF MEASUREMENT

The apparatus (Fig. 1) consists of the experimental chamber 2 and the associated electronic equipment. Inside the chamber a vacuum of $\sim 10^{-6}$ torr is maintained with a type TsVL-100 diffusion pump, a type RVN-20 fore vacuum pump, and a liquid nitrogen trap. In the chamber are placed a source of fission fragments and α particles 1, the target being studied 6, a semiconduc-

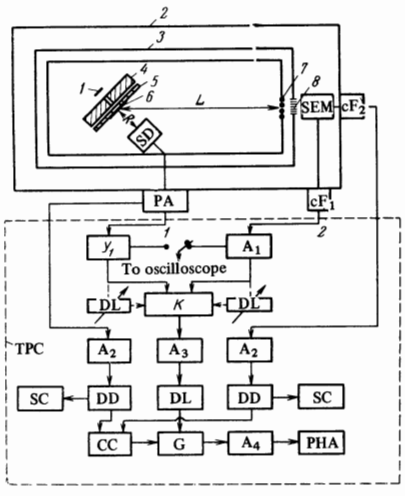

FIG. 1. Diagram of experimental equipment (the designations are explained in the text). DL—delay line.

tor detector SD of the surface-barrier type for detection of fission fragments and α particles, and a secondary electron multiplier SEM of the open type for detection of electrons.

In order to avoid bending of the secondary electron paths by the Earth's magnetic field and other magnetic fields, the electron drift space is surrounded by a double magnetic shield 3 in the form of a separable cylindrical enclosure of annealed mark 79NM Permalloy with a screening coefficient of ~110. In the end of the magnetic shield an opening is provided so that electrons can reach the SEM, which is covered by two grids: the internal grid 7, which is plane and has a transparency of 90%, and the external grid 8, which is of the venetian blind type, for focusing the electron beam onto the SEM, which is prepared as described by Baldwin.[8] On the internal surface of the internal cylinder of the magnetic screen with the grid a layer of aluminum was deposited by vacuum evaporation, and the SD and radioactive source were placed in an aluminum foil shield to avoid the effect of contact difference of potential.

The source of primary particles (fission fragments and α particles) is a thin layer of the spontaneously fissile isotope Cf^{252}, deposited on a polished tantalum substrate. The layer is covered on top with a film of lacquer no more than 50 $\mu g/cm^2$ thick to avoid sputtering of Cf^{252} atoms. The target under study is a layer of Al 25 $\mu g/cm^2$ thick, deposited by vacuum evaporation on a film of Al_2O_3 50 $\mu g/cm^2$ thick, which in turn is mounted on a ring 5. A beam of fission fragments and α particles 1.5 mm in diameter, defined by collimator 4, passes through the layer of Al and is detected by the SD, which is located at a distance R = 40 mm from the target, and the electrons corresponding to them, emitted from the Al, enter the flight path shielded from electric and magnetic fields; a part of them, after traveling a distance L = 82 mm, reached the opening in the Permalloy shield, and are accelerated and detected by the SEM. The angle between the direction in which the detected electrons are emitted from the Al and the direction of the primary particles is $45° \pm 2°$.

The distribution of delay times $N(\tau)$ of the stop signals (pulses from the SEM due to secondary electrons) with respect to the start signals (pulses from the SD due to the primary particles, which mark the time of emission from the aluminum foil) allows us to determine the secondary electron energy spectrum N(E), which is related to $N(\tau)$ by the equation

$$N(E) = N(\tau)\, d\tau / dE.$$

The delay time τ is measured by the time-to-pulse-height converter TPC (enclosed by the dashed line in Fig. 1). The negative pulse produced by the primary particle in the semiconductor detector SD is amplified by the preamplifier PA and fed to input 1 of the main channel of the TPC. Input 2 of the TPC receives the pulse produced by the secondary electron in the collector of the SEM, which is transmitted through the cathode follower CF_1. Both of these pulses are amplified by wide band amplifiers A_1 and are fed to the converter C, where a linear conversion of the delay time between these pulses to pulse height is performed by the overlap method.[10] The pulses from the converter are amplified by linear amplifier A_3, passed through linear gate G which is opened by pulses from coincidence circuit CC, and output amplifer A_4, and are analyzed by the pulse height analyzer PHA (AI-100-1). Positive pulses from the preamplifier and from the last dynode of the SEM (through cathode follower CF_2) are fed to the corresponding auxiliary channels of the TPC, which consist of linear amplifiers A_2 and differential discriminators DD. The threshold of the DD in the SD auxiliary channel is chosen so that the coincidence circuit receives pulses either from fragments or from α particles. In the SEM auxiliary channel the lower threshold of the DD is set to discriminate against pulses from single electrons with amplitudes less than the threshold for definite operation of the converter C.

Thus, in the pulse height analyzer PHA a distribution is obtained of the time of flight $N(\tau)$ of the secondary electrons produced either by α particles or by fission fragments, as a function of the discrimination levels of the DD in the SD auxiliary channel. The oscilloscope and the scaling circuit SC serve to monitor the spectrometer operation during the measurement. In addition, the SC performs other functions. Thus, the ratio of the rate of arrival of pulses at the PHA to the counting rate of the SC in the SD channel characterizes the SEE coefficient of the corresponding primary particle, and the dependence of the SC counting rate in the SEM channel on the accelerating voltage V_{acc} between grid 8 (Fig. 1) and the SEM is the counting-rate characteristic of the SEM channel. Figure 2 shows a curve taken in this way of the SEM counting characteristic for a SEM supply voltage of 3.8 kV.

The useful range of the time-to-pulse-height converter described is 5–300 nsec. The physical time resolution of the spectrometer and the time zero for experiments with fission fragments were determined from the coincidence peak for pulses from the two fragments of the isotope Cf^{252}, deposited on an Al_2O_3 substrate 50 $\mu g/cm^2$ thick. It turned out to be 14 nsec.

Calibration of the spectrometer time scale in the experiment with α particles was accomplished as follows. First the spectrum was recorded for a value of V_{acc} providing the same efficiency for detection of sec-

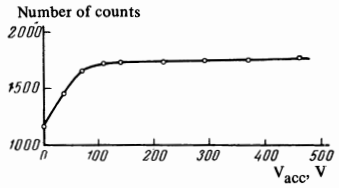

FIG. 2. Secondary electron multiplier counting characteristic.

ondary electrons regardless of their energy, i.e., the data were taken on the plateau of the SEM counting characteristic. Then the spectrum was recorded for the same length of time but without the accelerating voltage V_{acc}. The energy at which these two spectra become the same obviously corresponds to the voltage V_{acc} at which the SEM counting characteristic reaches a plateau. The differential nonlinearity of the spectrometer turned out to be 2% or less.

3. EXPERIMENTAL RESULTS AND DISCUSSION

Figure 3 shows energy distribution curves obtained by the method described above for secondary electrons due to α particles (curve 1) and due to fission fragments (curve 3). The value of N(E) at the peak is taken as unity. It is evident that the most probable energy E_{max} of secondary electrons in the α-particle case is 1.8 eV, and in the fission-fragment case, 0.3 eV. The ratio of the SEE coefficients of fission fragments and α particles, measured by the method described above, turned out to be 22. We will attempt to make clear to what extent the experimental data obtained correspond to a thermal mechanism of SEE.

It is well known that charged fission fragments, passing through matter, produce strong local heating in regions surrounding the track of these fragments (thermal spike), which is associated with the energy transferred to the medium by the fission fragments. The main part of the fragment energy is transferred to electrons (more than 90%) and only a few per cent to the lattice. The energy received by the electrons can be transferred only extremely slowly to the lattice because, in the last analysis, of the small ratio of the electron mass to the mass of the lattice.

For rather high temperatures ($\sim 10^4$ °K) the duration of electron-electron collisions (10^{-14} sec) turns out to be much smaller than the duration of electron-phonon collisions (10^{-11} sec),[11] which can result in establishment of two temperatures: an electron temperature and a lattice temperature. To determine the temperature in the region of a thermal spike, we can use the heat conduction equation. Establishment of a high electron temperature can lead to an increase in thermionic emission. We will assume that the energy distribution of the electrons is in thermodynamic equilibrium with the temperature T, whose value at each point of the medium is determined by heat conduction from instantaneous heat sources—thermal spikes. Then the thermionic emission current resulting from bombardment of the sample by fission fragments, under the assumptions made, can be computed from the formula

$$I = \int_{T_0}^{T_{max}} I(T)\,P(T)\,dT, \qquad (1)$$

where P(T) is the probability density that as the result

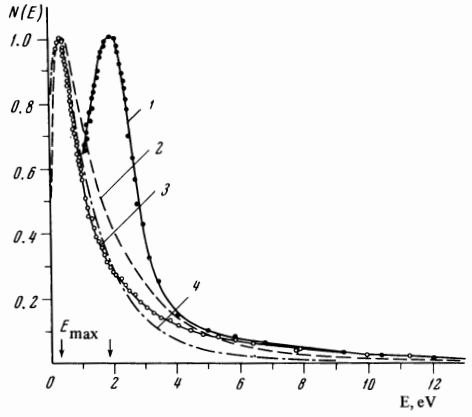

FIG. 3. Energy spectra of secondary electrons.

of local heating the electron temperature at a given point of the sample will be higher than T, I(T) is the function determined by the Richardson equation, T_0 is the sample temperature before the bombardment, and T_{max} is the maximum electron gas temperature occurring in the fragment tracks.

A method of calculating P(T) was developed by I. Lifshitz.[12] Subsequently the function P(T) was calculated on the basis of his results for study of the variation of the volume properties of crystals under the action of fission fragments.[13] In order to discuss electron emission from the surface of metals, in claculating P(T) it is necessary to take into account surface heat losses due to radiation, in accordance with the Stefan-Boltzmann law. This fact considerably complicates the calculation of P(T). Since we are here interested in the function P(T) in the rather high temperature region ($T \gg \overline{T}$, where $\overline{T}$ is the average temperature in the sample), we will use an approximate procedure which is actually based on dimensional considerations. In the case being discussed the temperature gradients along the fragment track direction can be assumed small in comparison with the temperature gradients in the plane perpendicular to the fragment track. With this assumption the heat conduction equation becomes two-dimensional and, when we include the heat loss by radiation, takes the form

$$c(T)\frac{\partial T}{\partial t} = \varkappa\left(\frac{\partial^2 T}{\partial \rho^2} + \frac{1}{\rho}\frac{\partial T}{\partial \rho}\right) - \frac{2\sigma T^4}{L}, \qquad (2)$$

where c(T) and κ(T) are the heat capacity of a unit volume and the thermal conductivity of the electron subsystem, L is the thickness of the foil, and σ is the constant entering into the Stefan-Boltzmann law.

Now let $\rho(t)$ be the radius of a cylindrical region surrounding the fragment track, inside which the average temperature is T(t). Since approximately

$$\frac{\partial^2 T}{\partial \rho^2} + \frac{1}{\rho}\frac{\partial T}{\partial \rho} \sim \frac{T}{\rho^2(t)}$$

and, furthermore

$$\rho^2(t) \sim \chi(T)t,$$

where $\chi(T) \equiv \kappa/c(T)$ is the temperature conductivity, then Eq. (2) can be approximately written in the following form:

$$c(T)\frac{\partial T}{\partial t} \approx \varkappa\frac{T}{\rho^2(t)} - \frac{2\sigma T^4}{L}. \qquad (3)$$

If the electron and lattice temperatures are the same, then in (2) and (3) for temperatures greater than the Debye temperature we can assume c = const and κ = const. If the electron temperature T_e considerably exceeds the lattice temperature T_L, then for discussion of thermal relaxation in the electron subsystem, it is necessary to assume in (2) and (3) that $c(T) \sim T_e$ (in the case of weak degeneracy of the electron gas), while κ is in this case some, generally speaking, complicated function of T_e. Actually, since $\kappa \sim c(T_e)\lambda_{eff}v_e$, where λ_{eff} is the electron mean free path due to scattering of electrons by photons, and v_e is the electron velocity at the Fermi surface, then for $T_L > T_D$ (T_D is the Debye temperature), $\lambda_{eff} \sim 1/T_L$ and $\kappa(T_e) \sim T_e/T_L(T_e)$. Since we do not know a priori which regions of the track are responsible for the main quantity of electrons emitted from the crystal, in the future, in addition to c = const and κ = const, we will consider also the case $c \sim T_e$, κ = const. Since $T_L(T_e)$ is an increasing function of T_e, the assumption κ = const in the presence of two temperatures is only the simplest approximation, which is strictly justified only in the case when $T_L \sim T_e$.

For small times t the solution of equation (3) can be sought in the form $T(t) \sim 1/t^s$. Substituting this relation into (3) and taking into account that $\rho^2(t) \sim \kappa t/c(T)$, we find that $s = 1/2$, if $c(T) \sim T$, κ = const, and $s = 1/3$, if c = const, κ = const.

Let us now define a volume $\omega(T)$ of a four-dimensional region in which the temperature is higher than a given T:

$$\omega(T) = \pi L \int_0^t \rho^2(t')\,dt' = \sim \begin{cases} t^{3/2} \sim T^{-5} & \text{for } c \sim T,\ \varkappa = \text{const} \\ t^2 \sim T^{-6} & \text{for } c = \text{const},\ \varkappa = \text{const} \end{cases}.$$

According to Lifshitz,[12] the desired function is $P(T) = -d\omega/dT$. Consequently, in regions of large T

$$P(T) \sim \begin{cases} 1/T^6 & \text{for } c \sim T,\ \varkappa = \text{const} \\ 1/T^7 & \text{for } c = \text{const},\ \varkappa = \text{const} \end{cases}. \quad (4)$$

We note that if we do not take into account heat loss by radiation and omit in (2) the term corresponding to the heat sink associated with loss by radiation, the value of s, which determines the function T(t) (see above), cannot be determined from the approximate equation (3) (this equation is satisfied for any s). In this case it is possible to use the heat balance equation

$$L\pi\rho^2(t)c(T)T \approx Q_0,$$

where Q_0 is the energy transferred by the fragment to the electron subsystem, and L is the fragment track length. Again taking into account that $\rho^2(t) \sim \kappa t/c(T)$, for κ = const we find that $T(t) \sim 1/T$, so that $P(t) \sim 1/T^4$ if $c(T) \sim T$ and $P(T) \sim 1/T^3$ for c = const, which agrees with the result of the exact solution found by Lifshitz et al.[13]

The more rapid drop of the function P(T) with increasing T when radiation losses are taken into account has an obvious physical meaning and is associated with the fact that this loss is unimportant only for small T.

Using the expression found for P(T) and performing the integration in (1) we can obtain the following expression for I (for c = const, κ = const, and without inclusion of losses by radiation):

$$I = I_0(\bar{T}) + I_1, \quad I_1 = Bq^2\Phi;$$

here $I_0(\bar{T})$ is the Richardson current of a sample whose average temperature is $\bar{T}$, while I_1 is the current due to deviation of the temperature T from $\bar{T}$; B is some function of the thermal conductivity and heat capacity of the electron gas; Φ is the flux of fission fragments; q is the energy loss by the fragment per unit path length. Under conditions when the average temperature of the sample is small in the presence of rather intense heat dissipation, the thermionic emission current is due mainly to I_1, i.e., $I \approx Bq^2\Phi$. Hence it follows that the secondary electron emission coefficient $\Delta = I/\Phi$ is determined by the relation

$$\Delta \approx Bq^2, \quad (5)$$

i.e., is proportional to the square of the specific ionization loss.

Let us turn now to discussion of the energy spectrum of the emitted electrons. If the temperature of the electron gas is T, then the number of electrons emitted at angle θ to the normal to the surface of the metal with energy ϵ, in the interval ϵ, $\epsilon + d\epsilon$, is

$$N(\varepsilon) = \frac{4m}{2\pi\hbar^3}\frac{[1-R(\varepsilon)]\varepsilon}{e^{(\varepsilon-\mu)/T}+1}\cos\theta\, d\Omega \equiv A\frac{[1-R(\varepsilon)]\varepsilon}{e^{(\varepsilon-\mu)/T}+1} \quad (6)$$

where m is the effective mass of the electron in the metal, $R(\epsilon)$ is the reflection coefficient of an electron with energy ϵ from the potential barrier, μ is the chemical potenial of the electrons, and $d\Omega$ is the solid angle in which the secondary electrons are detected. The energy ϵ is measured from the bottom of the conduction band of the metal. The existence of the thermal spikes leads to the fact that the temperature at an arbitrary point of the metal is a random quantity described below by the probability density P(T) (see Lifshitz[12]). Therefore expression (6) must averaged by means of the function P(T). The result of this averaging has the form

$$\overline{N(\varepsilon)} = A[1-R(\varepsilon)]\varepsilon\int_{T_0}^{\infty}\frac{P(T)\,dT}{e^{(\varepsilon-\mu)/T}+1}$$

$$= A[1-R(\varepsilon)]\varepsilon(\varepsilon-\mu)\int_{T_0/(\varepsilon-\mu)}\frac{P((\varepsilon-\mu)x)\,dx}{e^{1/x}+1}, \quad (7)$$

where T_0 is the target temperature before bombardment. Here we assume that for the temperatures of the thermal spikes which provide the main contribution to the integral in the right side of Eq. (7), the quantity μ can be considered weakly dependent on temperature. This assumption is clearly valid for those metals in which $\mu \gg E_{av}$, where E_{av} is the average energy of the electrons in the SEE spectrum. Since for the energy region of interest to us, $\epsilon \geq \mu + \varphi$, the condition $T_0/(\epsilon - \mu) \lesssim T_0/\varphi \ll 1$ is satisfied, where φ is the work function, then in formula (7) as the result of the rapid falloff of the function $e^{-1/x}$ at small x the lower limit of integration can be taken as zero. For the same reason the value of the integral in Eq. (7) is sensitive to the behavior of the function P(T) only for large values of the argument.

If the energy of the emitted electron E is computed with respect to the level of an electron at rest in vacuum $E = \epsilon - U_0$, where U_0 is the depth of the potential well for electrons in the metal, then Eq. (7) with inclusion of (4), for the case $P(T) \sim 1/T^n$ (see Eq. (4)), can be written in the form

$$N(E) \sim [1 - R(E - U_0)] \frac{E + U_0}{(E + \varphi)^{n-1}} \int_0^\infty \frac{dx}{(e^{1/x} + 1) x^n}$$

$$\sim \frac{[1 - R(E + U_0)](E + U_0)}{(E + \varphi)^{n-1}}, \quad (8)$$

where $\varphi = U_0 - \mu$ is the work function for removal of an electron from the metal. The reflection coefficient appearing in Eq. (8) for an electron of energy E depends on the shape of the potential barrier. For a square potential well of depth U_0 the barrier penetration coefficient is

$$1 - R(E + U_0) = 4\sqrt{E(E + U_0)} / (\sqrt{E} + \sqrt{E + U_0})^2.$$

In this case the energy spectrum has the form

$$N(E) \sim \frac{4E^{1/2}(E + U_0)^{3/2}}{(E + \varphi)^{n-1}[E^{1/2} + (E + U_0)^{1/2}]^2}, \quad (9)$$

i.e., for $E \ll \varphi$ the energy distribution approaches zero according to a $\sqrt{E}$ law.

Equation (9) describes a curve with a maximum at E_{max}, whose position for $E_{max} \ll U_0$ is determined by the relation

$$E_{max} = \varphi / (2n - 3). \quad (10)$$

Since for Al the work function is $\varphi = 4.25$ eV, we obtain according to (10) and (4), $E_{max} = 0.47$ eV for n = 6 and $E_{max} = 0.38$ eV for n = 7.

In Fig. 3 in addition to the experimental curves we have shown theoretical curves and 2 and 4 (respectively n = 6 and 7), calculated from formula (9). If we take into account the approximate nature of the calculations and also the possible experimental errors and the large spread in values of φ for Al (see [4]), the agreement of the theoretical and experimental results can be regarded as satisfactory, which argues in favor of the validity of the thermal mechanism of secondary electron emission for fission fragments. Since the average energy of thermionic electrons is $E_{av} \approx 2kT$, the average electron temperature in the thermal spike from fission fragments turns out to be $kT \approx 0.2$ eV. It is necessary, however, to keep in mind that far from the surface of the film this temperature can be, in accordance with what has been said above, several times larger than at the surface. Since we are speaking here of the average electron temperature in regions of the medium far from the surface of the crystal, we have, as in previous work on the theory of thermal spikes, not taken into account the energy loss of the electrons by radiation. Since in the temperature region $kT \sim 5$–10 eV the wavelength of electromagnetic radiation is of the order of 5000 Å, i.e., roughly two orders of magnitude larger than the track diameter which corresponds to the high electron temperatures, the radiation in practice is not reabsorbed in the medium and consequently leads to an additional loss, and not to an additional contribution to the electron gas heat conduction coefficient. We intend to discuss these losses specifically in the future. Here we only note that the effect cited above leads to a somewhat stronger dependence of the function P(T) on T and, consequently, to improved agreement between experiment and the theoretical shape of the secondary electron energy distribution.

At the same time it appears completely obvious to us that the emission mechanism in the case of α particles is something different. This conclusion is the same as that drawn by us previously.[3] Furthermore, if the SEE mechanism for α particles also had a thermal nature, then in accordance with Eq. (5) the ratio of SEE coefficients for fission fragments and α particles should be 400, whereas the experimental value of this ratio is 22. Although in Eq. (5) we have not taken into account radiation losses, their inclusion, which we are carrying out at the present time, will remove this discrepancy.

In conclusion we note that according to the thermal theory the angular distribution of the emitted electrons should follow a law $\partial N(\epsilon)/\partial\Omega \sim \cos\theta$ where θ is the angle between the electron emission direction and the normal to the foil, and Ω is the solid angle. In this connection it is of interest also to study the angular distribution of the secondary electrons.

We have mentioned above the possibility of establishing in the region of the thermal spike two, generally speaking, different temperatures: the electron gas temperature and the lattice temperature. Since the best agreement with experiment is obtained for the case c = const and κ = const, which leads to a dependence $P(T) \sim 1/T^7$, at least that portion of the secondary electrons which comprise the region of the peak of the N(E) curve apparently corresponds to a duration of the thermal spike such that the difference between the electron and lattice temperatures becomes unimportant.

In conclusion the authors thank A. I. Leĭpunskiĭ for his constant interest in this work and his support, and also Yu. Ya. Stavisskiĭ for helpful advice in discussion of the choice of experimental technique. The authors are grateful to Yu. V. Chmyrev for assistance in the work.

[1] P. L. Kapitza, Phil. Mag. 45, 989 (1923).
[2] E. J. Sternglass, Phys. Rev. 108, 1 (1957).
[3] V. M. Agranovich, D. K. Daukeev, Yu. V. Konobeev, S. Ya. Lebedev, Yu. Ya. Stavisskiĭ, and Yu. V. Chmyrev, Izv. AN SSSR, ser. fiz. 32, 5 (1969).
[4] J. N. Anno, J. Appl. Phys. 33, 1678 (1962).
[5] F. E. Jamerson, C. B. Leffert, and D. B. Rees, J. Appl. Phys. 36, 355 (1965).
[6] A. B. Whitehead, IEEE Trans. Nucl. Sci. (U.S.A.) 13, 747 (1966).
[7] W. E. Stein and R. B. Leachman, Rev. Sci. Instr. 27, 12 (1956).
[8] G. C. Baldwin, Rev. Sci. Instr. 38, 55 (1967).
[9] M. Y. Nakai, Rev. Sci. Instr. 38, 98 (1967).
[10] E. I. Rekhin, A. A. Kurashov, and P. S. Chernov, Izmerenie intervalov vremeni v eksperimental'noĭ fizike (Measurement of Time Intervals in Experimental Physics), Atomizdat, 1967.
[11] V. L. Ginzburg and V. L. Shabanskiĭ, Dokl. Akad. Nauk. SSSR 100, 3 (1955).
[12] I. M. Lifshitz, Dokl. Akad. Nauk. SSSR 109, 1119 (1956) [Sov. Phys. Doklady 1, 512 (1957)].
[13] I. M. Lifshitz, M. I. Kaganov, and L. V. Tanatarov, Atomnaya énergiya 6, 391 (1959).
[14] V. S. Fomenko, Emissionnye svoĭstva élementov i khimicheskikh soedineniĭ (Emission Properties of Elements and Chemical Compounds), AN USSR, 1961.

Translated by C. S. Robinson
46